www.czasopisma.pan.pl PAN www.journals.pan.pl

Arch. Min. Sci. **66** (2021), 4, 561-578

Electronic version (in color) of this paper is available: http://mining.archives.pl

DOI: https://doi.org/10.24425/ams.2021.139597

SRI CHANDRAHAS[1,2*], BHANWAR SINGH CHOUDHARY[1],
N.S.R. KRISHNA PRASAD[2], VENKATARAMAYYA MUSUNURI[2], K.K. RAO[3]

AN INVESTIGATION INTO THE EFFECT OF ROCKMASS PROPERTIES ON MEAN FRAGMENTATION

Desired rock fragmentation is the need of the hour, which influences the entire mining cycle. Thus, most engineering segments pay attention to rock fragmentation and neglect by-products like ground vibration and fly rock. Structural and mechanical properties of rock mass like joint spacing, joint angle, and compressive strength of rock pose a puzzling impact on both fragmentation and ground vibration. About 80% of explosive energy that gets wasted in producing ill effects can be positively optimised, with a new set of blast design parameters upon identifying the behaviour of rock mass properties. In this connection, this research aims to investigate the influence of joint spacing, joint angle, and compressive strength of rock on fragmentation and induced ground vibration. To accomplish this task, research was carried out at an opencast coal mine. It was discovered from this research that compressive strength, joint spacing, and joint angle have a significant effect on the mean fragmentation size (MFS) and peak particle velocity (PPV). With the increase in compressive strength, MFS explicit both increase and decrease trends whilst PPV increased with a specific increase in compressive strength of the rock. An increase in joint spacing triggers both increase and decrease trends in both MFS and PPV. While there is an increase in joint angle, MFS and PPV decrease.

Keywords: Mean fragment size (MFS), Peak particle velocity (PPV), Joint angle, Joint spacing, Protodyakonov strength index test, rock mass

I. Introduction

Rock fragmentation has a central influence on overproduction and mining costs. Blasting is one of the essential techniques for achieving desired rock fragmentation in all open cast mines.

[1] DEPARTMENT OF MINING ENGINEERING, IIT(ISM) DHANBAD, INDIA
[2] DEPARTMENT OF MINING ENGINEERING, MALLA REDDY ENGINEERING COLLEGE, HYDERABAD, INDIA
[3] MANAGER, UCIL MINE, KADAPA, INDIA

* Corresponding author: srichandru2009@gmail.com

The efficiency of the utilisation of explosive energy will contribute to significant improvement in fragmentation.

There are other undesirable effects of blasting with regard to safety, like ground vibration, fly rock, fumes and air blast, which create a nuisance to nearby residents. Improvements in blast performance can be obtained by balancing the explosive energy to the rock strength, optimum dimensions & geospatial position of blast hole and other blast design parameters. The optimisation also contributed to the synergy of fragmentation coupled with avoidance of harmful effects. Thus, creating harmony between the mining community and the general society.

The explosive energy utilisation that impacts rock fragmentation and induced ground vibration mainly depends on two sets of variables: rock mass properties and blast design parameters. The rock mass properties play a crucial role, and they are uncontrollable. The presence of geological discontinues in a rock mass impacts blasting and its rock fragmentation [1]. Peak Particle Velocity (PPV) is influenced by rock mass properties [2].

The examination of rock conditions helps the user to adopt suitable blast design parameters accordingly. Mean fragmentation Size (MFS) and PPV increase with the rise in the rock mass compressive strength [3]. Good compressive strength of rocks up to a point makes the explosive energy consumption in rock mass be at a maximum so that rock breakage and fragmentation yield economic results. On the other hand, high compressive strength prevents the absorption of seismic waves and transmit further. Thus, less attenuation in the propagation of the wave in the rock produces more PPV.

The higher frequency of joints in rock mass influence both mechanical properties and the dynamic response of rock mass [4[. The stress wave immediately slows down and attenuates when it encounters any discontinuity in a rock mass [5]. Therefore, researching the relation between the quality and quantity of rock joints and rock mass strength is of paramount importance [6]. Joint presence in rock formation poses an impact on rock MFS, as well as on the safety of a blast [7]. Many research studies revealed that the natural block size of rock mass has a significant influence on rock fragmentation [8-12]. Similarly, rock joints have a prominent effect on shockwave propagation after blasting [13]. The transmission of stress wave is more affected by open and filled joints rather than tight joints. Both the open and filled joints instigate an acoustic impedance discrepancy and make the stress waves return. Whenever a blast hole is intersected by an open joint, or there is more space between joints in the rock, the gases after explosion expand the joint by a wedging action, causing it to escape. If the joint expands from the blast hole wall to the face or top of the bench, poor fragmentation will result, and that place can neither be drilled and blasted again nor handled by direct digging due to the existence of large-sized boulders and toe. With the increasing joint gap size, the PPV pulse width and the amplitude reduce linearly as we move away from the site of the blast [14]. Similarly, natural spacing in unfilled joints obstructs the transmission of waves further. Filled joints create a path to disseminate seismic waves from one end to another. A void in the joint attenuates completely and is reflected when hitting the joint.

Many researchers derived their investigation with remarkable variations in stress wave propagation, fracture appearance and crushing area size on all sides of blast hole for open or filled and closed joints [15-17]. The amount of yield produced by the blast is also lower as the transmission of radial cracks is cut off by the cavities [18]. Gas pressure immediately decreases as the blasthole interchanges with space and stops the spreading of the fractures, while the gases runoff towards the gap in joints. The stress wave attenuation rate in joints depends on the incidence angle concerning the joint face [19-21]. In summary, rock joint spacing acts as a filter to stop seismic wave propagation.

Besides joint spacing, the effect of joint orientation on mean fragmentation size is also important [22,23]. In several cases, the rock fragmentation was significantly influenced by the direction of a blast with respect to the joint plane. Poor rock fragmentation resulted when the direction of wave propagation was oblique to the joint plane, and good rock fragmentation was obtained when the blast was parallel to the plane of weakness. Many cases revealed better fragmentation with the direction of the free face parallel to joint planes [24,25]. The shape of the cavity produced after the blast is influenced by the direction of the free face concerning its planes of weakness [26]. It was also indicated that rock fragmentation intensity and regularity in the fracture of the anisotropic form will be controlled by the orientation apropos to charge space and the free surface.

The joint angle also impacts ground vibration along with fragmentation. An increase in joint angle is capable of bringing change in attenuation rate of vibration velocity, thus change in joint angle has a good enough impact on the blast vibration [27]. The association between a blast stress wave and rock joint will depend on the touching angle, wave type, and mechanical characteristics of the joint that can dispel the blast energy [28-30]. A divergent angle regarding rock joint will source divergent stress wave attenuation. Generally, normal angle 900 causes the attenuation of stress waves to occur rapidly [31]. The transference coefficient repetitiously reduces with rising incident angle, while the backscatter coefficient rises evenly up to the incident angle and proceeds towards the critical angle at 900 [32]. Thus, the incident angle was affected by wave transference and backscattering.

2. Objectives of the study

- To investigate the effect of joint spacing, joint angle, and rock compressive strength on mean fragmentation size.
- To investigate the effect of joint spacing, joint angle and rock compressive strength on ground vibration (Peak particle velocity).

3. Field description & research methodology

To meet the objectives of the research, a field study was conducted at Opencast mine I, Ramagundam region III areas, Singareni collieries company limited, in Telangana, India. Twenty-six blasts data were obtained from six different benches in two phases viz fifteen blasts in phase-I and eleven blasts in phase II, collected from OB Shovel bench.

The study benches were 17 meters high. Rock strata were friable and consisted of sandstone and alluvium soil. The diameter of the blast hole was 250 mm and a depth of 18 meters. The explosive was Site Mixed Emulsion (SME). The drilling pattern was square, and the firing pattern was a line initiated with a cast booster and NONEL initiation system. The density of sandstone was 2.3 g/cc. The mine site, OB bench, Blast site, and Blast parameters measurements are shown in figures 1 to 4, respectively.

Blast design parameters, including a burden (m), spacing (m), blast hole length (m), blast hole diameter (mm), total explosive (kg), charge per hole (kg), stemming length (m), firing pattern and structural properties like joints, were collected during the initial visit. Every blast was photographed with a suitable camera in daylight to analyse fragments size in FRAGALYST

Fig. 1. Overall picture of mine from view point

Fig. 2. OB sandstone bench

Fig. 3. Blast site

Fig. 4. Burden & spacing measurement

SOFTWARE. Twenty-six trial blasts were conducted to observe the impact of joint spacing, joint angle, rock compressive strength on fragmentation and ground vibration in 20 days. The joint spacings were analysed, measured manually and using face photographs in FRAGALYST SOFTWARE. There were two sets of joints observed, one almost parallel to the horizontal and another vertical at faces.

The geological condition of rock mass was isotropic in all directions in the area. To maintain uniformity in the observations, vibration monitoring, in particular, the locations of the observation point were chosen at the same angle to the blast site. Any small effect of the differences in the angle has been ignored. The samples regarding rock properties were collected at the benches randomly at experimental drilling sites. Vibrations were monitored at distances 300-1500 m randomly from the blast site, using an engineering seismograph (MINIMATE).

A design of the blast is created using O-PITBLAST software. The design encompasses vibration attenuation and prediction. O-PITBLAST works on the RENISHAW laser 3D technique in transforming a view of the design into a multidimensional visualisation that brings a more realistic representation of the blast. Required software supporting files obtained from AUTOCAD 123D from converting 2D photographs into 3D coordinates. The blast hole charging length was 18 m, where the alternative explosive charge was 4.5 m, and decking & stemming was 1.5 m & 3.5 m, respectively. Similarly, the hole-hole delay used was 17 ms, and the row delay was 42 ms.

The decking was maintained six times to the hole diameter to avoid sympathetic detonation between two charges. Pattern simulation and blast hole charge are shown in figure 5 designed in O-PITBLAST.

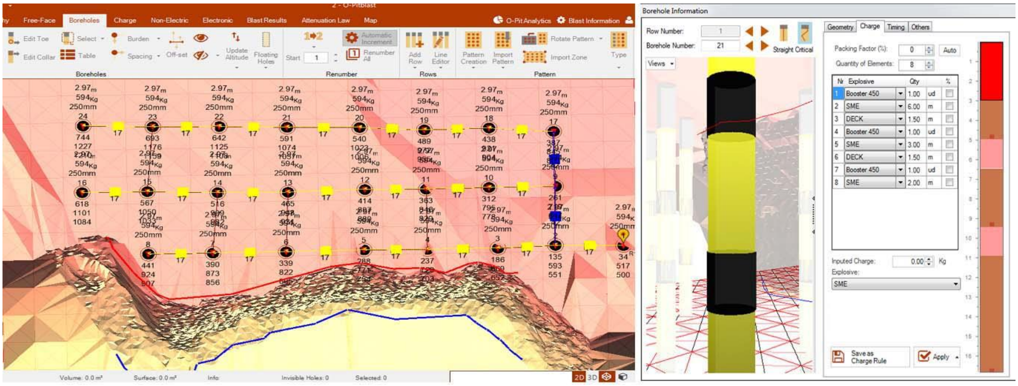

Fig. 5. Blast design in O-PITBLAST

All blast design parameters are synchronized by the software as per the actual structural and mechanical properties of the rock mass. The interface has the intelligence to check information like a flaw in connections, overcharge, burden distribution, hole inclination, stemming, deck misplacement, and structural problems within the vicinity of the blast. After correcting the discrepancies, the software allows the user for further analysis. The picture shown in figure 6 was iterated several times to avoid errors and arrive at a successful blast design.

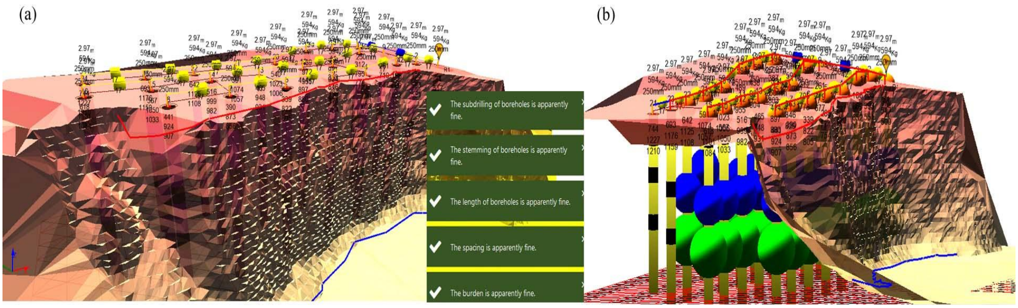

Fig. 6. Final design and software check for problems

3.1. Rock Compressive strength test

Protodyakonov strength index test gives compressive strength of rock material in a hassle-free manner. The apparatus shown in Fig. 7 is used to find the compressive strength of rock. Six sets of sandstone samples were collected between the blast hole site and observation area at random.

Weighing 100 g at a size range of $21 \geq 22$ mm, each of the samples were taken to a Protodyakonov strength index test apparatus. A 1.8 kg weighted plunger was dropped from a height of 0.64 m for 20 blows (n) which crushes material. The broken material was then moved into a 0.5 mm sieve.

Suitable rock pieces passing the sieve were poured into a volume-meter for measuring column height (h).

Protodyakonov strength index (PSI) test strength index value is then obtained from the formula.

PSI = 20 n/h. The relation between Protodyakonov strength index and compressive strength can be estimated with the relation UCS = PSI × 100 kg/cm^2.

Fig. 7. Protodyakonov strength index test apparatus

3.2. Joint analysis in FRAGALYST

FRAGALYST software was used for joint analyses and fragmentation analysis. Joint angle, spacing, and in-situ block size distribution (ISBD) curves are used to analyse joint influence, similarly, blasted block size distribution (BBSD) curves for fragmentation analyses. Initially, joints were analysed by image analysis using three steps 1) Photograph import and setting scale value b) Marking of joints on the photograph as per visual appearance c) Image delineation & ISBD Curve output.

ISBD is the assessment of the size of the naturally formed block. This is the block formed with the intersection of the joint faces. It is needed to be estimated to know its relation to the fragmentation desired and the effect on blast performance. The procedure for joint analysis is shown in Figs 8 to 9.

Fig. 8. Sandstone bench photographs

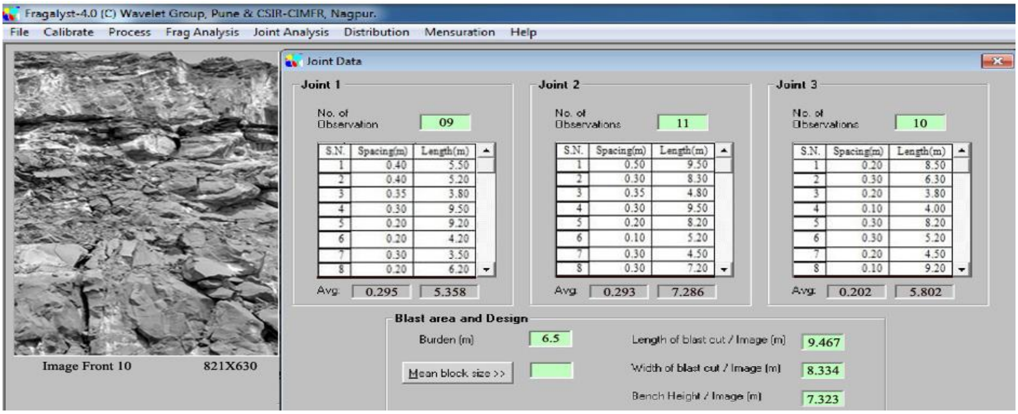

Fig. 9. Joint analysis in Fragalyst 4.0

3.3. Fragmentation analysis in FRAGALYST

For analysing rock particle size, the image analysis processing method was used in FRAGALYST software. The software works on the Rosin-Rammler model to analyse particle size distribution in this software. All bench face photographs were captured with a suitable camera; orange-coloured balls were used as an object for scaling purposes shown in figure 10(a). Initially, photographs were imported into FRAGALYST software and after a scale value was set. Upon threshold selection, edges of fragments detected as shown in figure 10(b), further image delineation process done as shown in figure 10(c) and then delineated images was sieved to obtain final BBSD curve shown in figure 10(d).

3.4. Ground Vibration Measurement:

The ground vibration was measured using an engineering seismograph, as shown in Fig. 11. To maintain direct contact with the Earth, a transducer is attached to spikes and are pushed firmly into the ground surface. The maximum charge per delay and measuring distances are 350 to 450 kgs

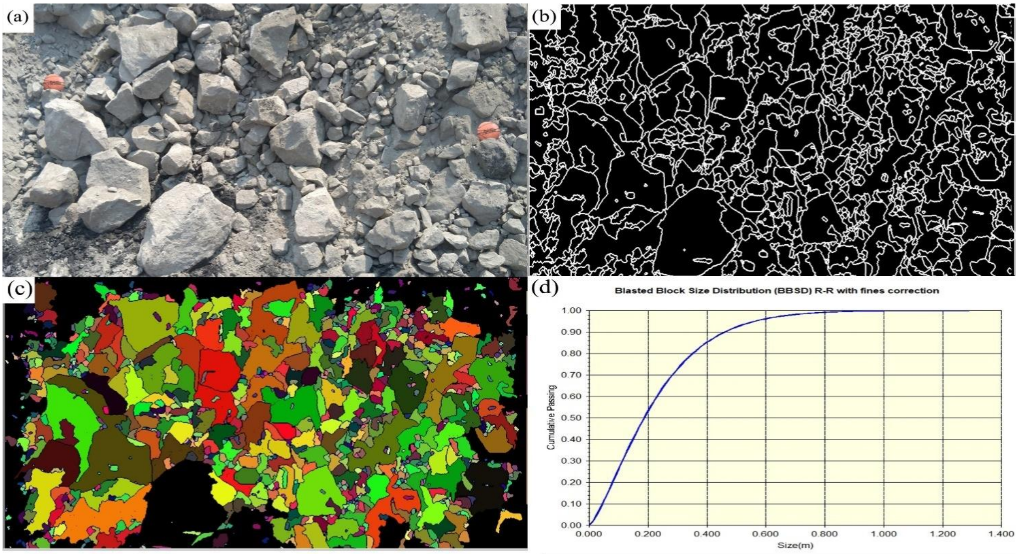

Fig. 10. (a) Imported photograph with scale, (b)&(c) Delineation of photograph, (d) BBSD Curve

and 300 to 1500 meters, respectively. For every blast, generated vibration data is exported and saved. During the blasts, the seismograph recorded PPV for longitudinal (R), vertical (V), and transverse (T) Components, vector sum velocity (VS) shown in the table.

Fig. 11. Seismograph measuring the ground vibration

The trends of PPV vis-a-vis scaled distances are shown in Fig. 12. The trends were generated based on monitored vibration data such as PPV and peak vector sums of transverse- longitudinal-

TABLE 1

Trial blasts design parameters

Blast No	Burden, m	Spacing, m	Average Hole Depth, m	Hole Diameter, mm	No. of holes	No. rows	Stemming Length, m	Average Explosive per hole, kg	Total Explosive, kg	PF, t/kg	Total Broken rock, t	Firing pattern
1.	6	8	16	250	30	5	3.5	540	16360	1.25	20535	line
2.	6	8	16	250	29	3	3.5	560	17300	1.09	18900	line
3.	6	8	19	250	30	5	3.5	670	16900	1.12	19006	line
4.	6	7	16	250	30	5	3.5	550	19500	1.09	19678	line
5.	6	7	16	250	30	5	3.5	540	16345	1.17	19134	line
6.	6	7	16	250	30	5	3.5	550	16300	1.25	20498	line
7.	6	7	18	250	30	5	3.5	620	16335	1.17	19144	line
8.	6	7	16	250	30	5	3.5	550	12900	1.50	19384	line
9.	6.5	8.5	16	250	30	5	3.5	560	12986	1.49	19367	line
10.	6.5	8.5	16	250	30	5	3.5	540	17890	1.16	20900	line
11.	6.5	8.5	17	250	30	5	3.5	605	16360	1.25	20535	line
12.	6.5	8.5	16	250	30	5	3.5	550	12600	1.53	19400	line
13.	6.5	8.5	16	250	30	5	3.5	550	17967	1.16	20970	line
14.	6.5	7.8	18	250	29	5	3.5	550	12900	1.50	19384	line
15.	6.5	7.8	19	250	28	5	3.5	680	12976	1.49	19350	line
16.	6.5	7.8	17	250	28	5	3.5	600	17650	1.84	20900	line
17.	6.5	7.8	17	250	28	5	3.5	600	16360	1.25	20535	line
18.	6.5	7.5	19	250	27	5	3.5	670	12600	1.53	19400	line
19.	6.5	7.5	17	250	27	3	3.3	590	12826	0.96	19200	line
20.	6.5	7.5	19	250	28	5	3.5	670	12986	1.49	19367	line
21.	6.5	7.5	16	250	27	5	3.5	540	16430	1.24	20400	line
22.	6.5	7.5	16	250	26	3	3.5	550	17350	1.08	18800	line
23.	6.5	8	16	250	27	5	3.5	545	19500	1.09	19678	line
24.	6.5	8	16	250	27	5	3.5	550	16345	1.17	19134	line
25.	6.5	8	16	250	26	5	3.5	550	16300	1.25	20498	line
26.	6.5	8	16	250	26	5	3.5	535	16335	1.17	19144	line

TABLE 2

Trial blasts results

S.No	Longi-tudinal mm/sec	Vertical, mm/sec	Transverse, mm/sec	PPV, mm/sec	PVS, mm/sec	Joint Spacing, m	Joint Angle, degree	Compressive Strength Kg/cm^2	Max Charge/ Delay, kg	Distance, m	BBSD, mm	ISBD, mm	Predicted PPV with same distance, mm/sec
1.	7.89	9.22	9.22	9.22	15.2	0.245	21	2970	430	300	190	950	9.60
2.	7.55	6.66	6.78	7.55	12.13	0.55	22	2950	360	400	230	950	6.13
3.	5.70	6.89	6.89	6.89	11.2	0.355	20	2850	450	500	175	960	5.28
4.	3.56	4.05	4.56	4.56	7.06	0.546	22	2820	360	600	185	860	3.70
5.	3.67	4.89	4.89	4.89	7.82	0.456	21	2800	360	700	170	900	3.09
6.	2.77	3.01	3.01	3.01	5.07	0.342	30	2750	360	800	190	1160	2.63
7.	1.69	1.01	1.01	1.69	2.21	0.325	22	2600	430	900	165	1060	2.05
8.	1.4	1.03	1.09	1.4	2.05	0.342	25	2570	360	1000	155	900	2.00
9.	2.98	3.09	3.09	3.09	5.28	0.34	25	2800	360	1100	140	670	1.78
10.	2.50	2.98	2.98	2.98	4.96	0.345	30	2700	360	1200	140	650	1.60
11.	2.13	2.05	2.05	2.13	4.12	0.55	25	2550	410	1300	130	760	1.56
12.	1.90	1.85	1.56	1.90	3.07	0.55	30	2400	360	1400	110	1050	1.33
13.	21.56	20.30	20.30	21.56	35.9	0.342	30	2600	370	200	100	960	19.80
14.	9.30	9.01	9.01	9.30	15.7	0.147	20	3250	480	300	190	680	10.20
15.	8.55	9.06	9.08	9.08	15.4	0.225	22	2950	450	400	180	690	8.30
16.	8.34	8.06	8.06	8.34	14.1	0.228	22	2960	430	500	180	500	5.10
17.	6.78	6.07	6.09	6.78	10.9	0.233	22	2900	420	600	175	600	5.70
18.	5.77	5.04	5.04	5.77	9.17	0.242	22	2890	450	700	175	920	3.50
19.	5.01	5.01	5.08	5.08	8.71	0.25	20	2800	470	800	165	800	3.90
20.	4.78	3.88	3.88	4.78	7.2	0.267	22	2800	460	900	165	680	2.60
21.	3.02	3.33	3.33	3.33	5.59	0.303	28	2750	360	1000	160	700	2.50
22.	3.00	3.01	3.01	3.01	5.2	0.322	21	2730	350	1100	160	500	1.75
23.	2.20	2.70	2.70	2.70	4.4	0.356	28	2710	360	1200	150	500	1.60
24.	2.03	1.96	1.96	2.03	3.43	0.365	30	2500	350	1300	150	580	1.40
25.	1.85	1.50	1.60	1.85	2.8	0.522	30	2500	360	1400	145	700	1.33
26.	1.87	1.50	1.85	1.87	2.8	0.594	28	2500	350	1500	140	500	1.20

vector directions, the maximum charge per delay, and measured distances in the software. The method used for the regression model was the least-squares method with logarithmic mode. Regression executed with the confidence levels of 50% and 95% for determinating the blast vibration estimation in the best fit.

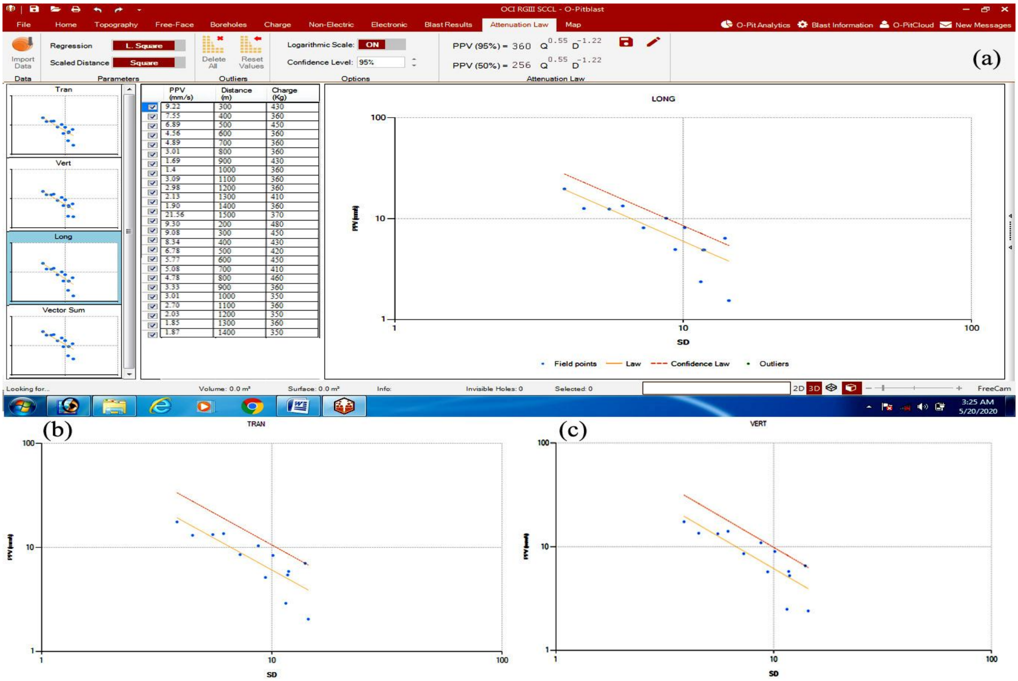

Fig. 12(a-c). Trends of PPV and scaled distance for longitudinal, transverse and vertical in O-PITBLAST

Figures 12(a-c) shows the relationship obtained between the scale distance (SD) and PPVs based on the attenuation equation presented in equation (A&B). The trend shows a clear direct relation that exists among the variables. PPV decreases with an increase in scaled distance (distance and maximum instantaneous charge) in all three directions longitudinal, transverse and vertical.

New attenuation law produced by a least-squares method based on Charles H. Dowding (1985) Equation (1).

$$U = a(R/W^{1/2})^m \tag{1}$$

Where

U — Peak particle velocity,
R — Distance from blast,
W — Maximum instantaneous charge,
SD — Squared Distance
a, m — Terrain influence factors,
$SD = R/W^{1/2}$

Using equation (1) modified attenuation law created by software for OCI, RGIII, SCCL shown in equations (A&B) with confidence levels 95% and 50% respectively.

$$PPV\,(95\%) = 360\; Q^{0.55}\; D^{-1.22} \tag{2}$$

$$PPV\,(50\%) = 225\; Q^{0.55} D^{-1.22} \tag{3}$$

Hence new site constants at 95% confidence level for the study site were K: 360, α: 0.55, β: –1.22K, α and β are Terrain influence factors

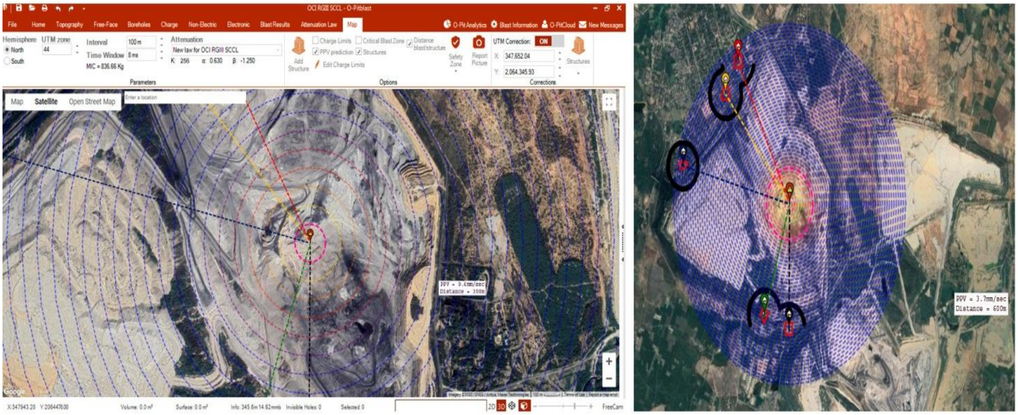

Fig. 13. PPV predicted values in O-Pitblast

Figure 13 is showing the contours of vibration both the monitored and predicted. The predicted values are close to real values as given in table 2.

4. Results and discussions

4.1. Relation between rock property and fragmentation

The relationship between various blast design parameters and results derived from the table 2 are given in figure 14(a-d).

It is evident from Fig. 14(a) that as the compressive strength increases the ranges between 2000 kg/cm^2 and 23350 kg/cm^2 (with an increase in UCS), the MFS also increases, which is similar to the other studies. To maintain the required MFS, it is necessary to understand the rock strength and accordingly plan for the blast design parameters.

The increase in rock strength It is well known that due to compactness of rock mass increased that resulted in better utilisation of explosive energy. However, when the compressive strength increased from 2350 kg/cm^2 to 3250 kg/cm^2, it improved the dynamic properties of the rock mass. Thus the MFS increases.

The graph clearly depicts in Fig. 14(b) that the dynamic response of the rockmass was influenced by the frequency of the fractures. When joint spacing increased from 0.20 m to 0.45 m

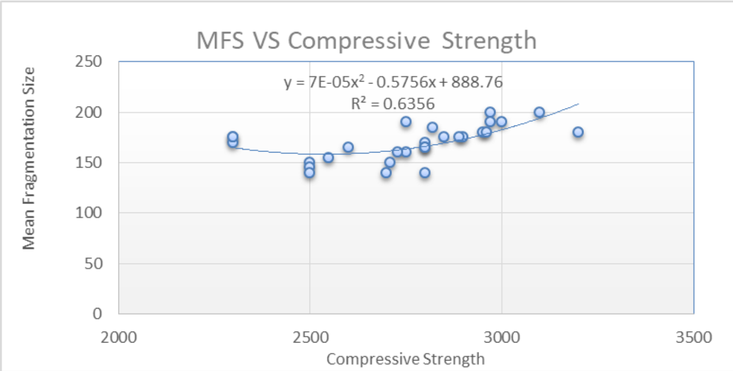

Fig. 14(a). Relation between MFS & Compressive Strength

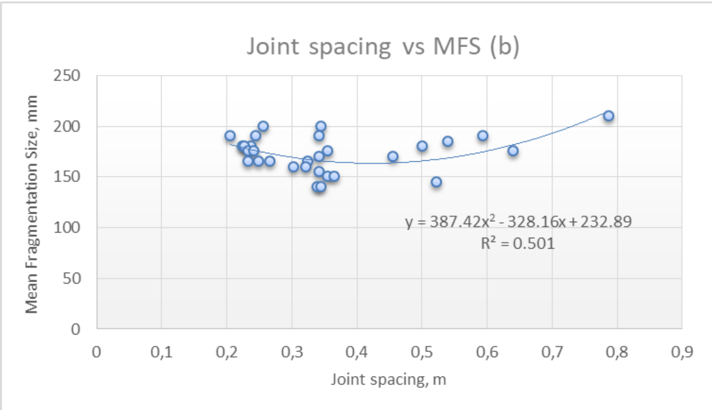

Fig. 14(b). Relation between MFS & Joint Spacing

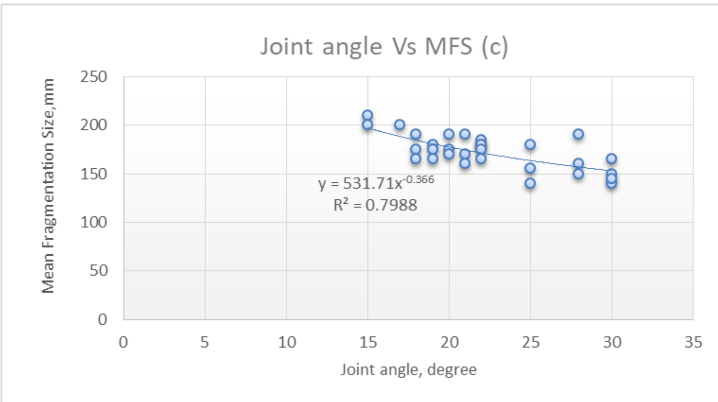

Fig. 14(c). Relation between MFS & Joint angle (number of joints per length, decreasing), the MFS showed a decreasing trend. This trend may be due to less wastage of explosive energy through cracks and joints. While the joint space increased beyond 0.45 m to 0.8 m (number of joints further increasing), the MFS also increased due to the improved rock mass conditions.

It is evident from Fig. 14(c) that as the joint angle rises, the MFS reduces gradually.This is due to the decrease in the in-situ block sizes with respect to the location of blast holes.

From Fig. 14(d), it is evident that the in-situ block size distribution (ISBD) has a direct relation with the Blasted block size distribution(BBSD). As the ISBD increases, the BBSD also increases. Here the phenomenon is observed, the change in the utilisation of explosive energy to the structural features of the rock mass.

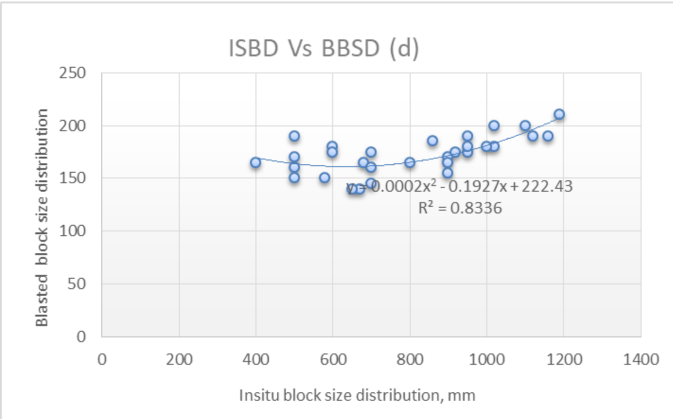

Fig. 14(d). Relation between BBSD & ISBD

4.2. Relation between rock property and ground vibration

The relationship between various blast design parameters and results are derived from table 2 and given in figure 15(a-e).

It is evident from Fig. 15(a) that as the compressive strength of rock increases, the PPV also increases. Initially, the curve showed a slight increase in PPV, this was due to the rock mass joints absorbing some of the vibrations, probably from the effect of the joints in the rockmass. After a certain point, the PPV is increased as the UCS does because of reduction in the joints high rock compressive strength acted as a scaffold to PPV for forwarding ahead without any interruption.

The graph drawn between PPV and Joint spacing in Fig. 15(b) reveals a negative relationship at lower joint spacing. At a joint spacing of 0.15 m to 0.40 m, PPV is reducing linearly with the increase in the joint spacing (less number of joints in unit length). The reason for this reduction in PPV could be understood as attenuation due to joints. Later at a joint spacing of about 0.45 m to 0.60 m, the PPV is increasing. There is less attenuation because there are fewer interruptions along linear dimensions. The increase in joint space also has the effect of an increase in compressive strength.

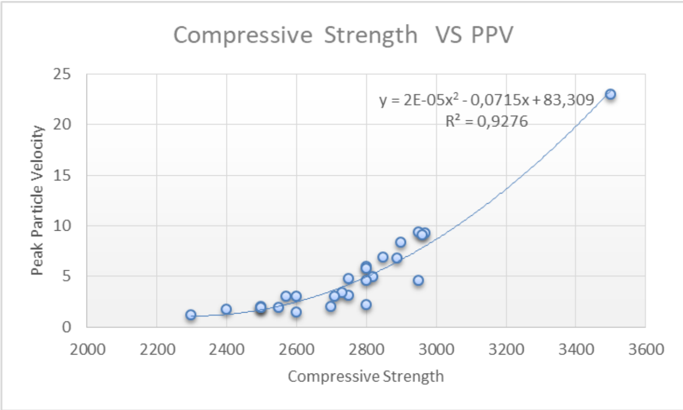

Fig. 15(a). Relation between PPV & Compressive Strength

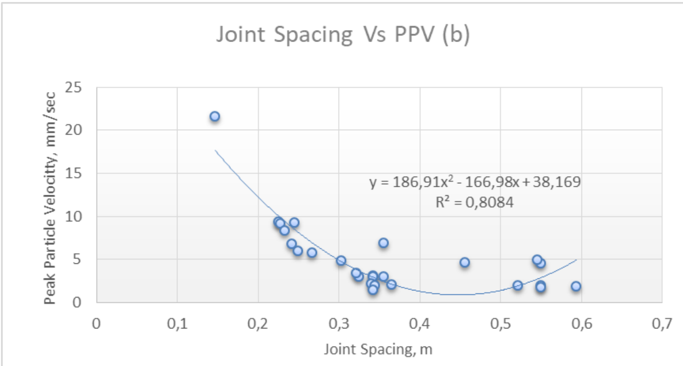

Fig. 15(b). Relation between PPV & Joint Spacing

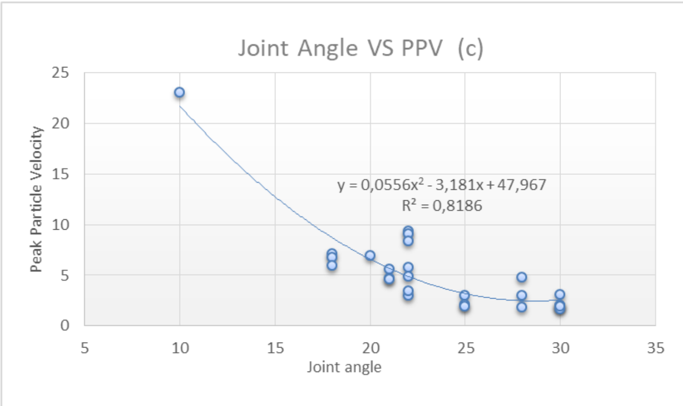

Fig. 15(c). Relation between PPV & Joint angle

As Fig. 15(c) shows, when the joint angle increases, the PPV decreases. The joint angle affects the layer of rock in which elastic waves reflect, and therefore the receiving PPV transmission is reduced.

From Fig. 15(d), it is evident that the maximum charge per delay (MCPD) in the range of 350 kg to 380 kg, the PPV is almost constant. This is because, at this range, the energy liberated from the explosive is mostly utilised in breaking the rock or getting dissipated. Thus there is not much increase in PPV. Beyond 400 kg of MCPD, the PPV is increasing linearly as the MCPD increases.

It is evident from Fig. 15(e) that the PPV level is very high nearer to the blasting area and slowly reduces as distance increases. It is because of the dissipation of energy in the rock mass with distance. The linearity of the dissipation shows that the rock is isotropic in nature around the blast area.

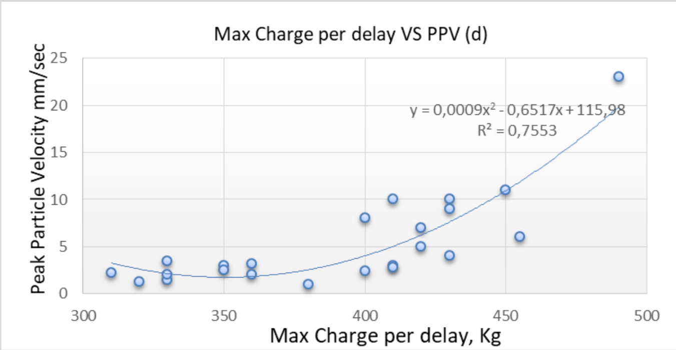

Fig. 15(d). Relation between Maximum Charge per delay & PPV

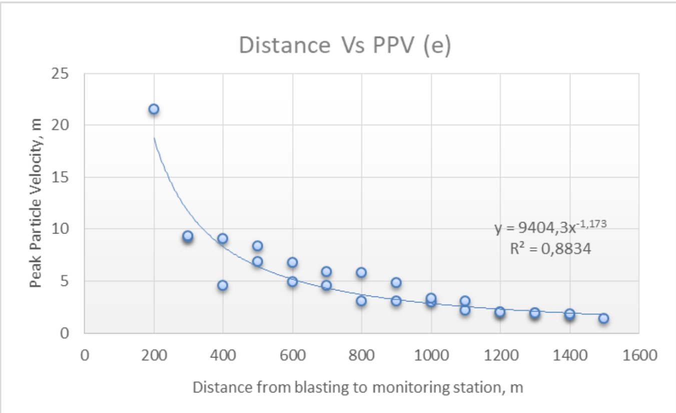

Fig. 15(e). Relation between distance & PPV

5. Conclusions

The following can be concluded from the study:

- The increases in rock compressive strength are shown in two variant trends, such as increase and decrease in MFS. PPV constantly increases with an increase in the compressive strength of the rock.
- Joint spacing increases show two variant trends, such as increase and decrease in both MFS and PPV.
- As the joint angle increases, MFS and PPV decrease.
- Mean fragmentation size and ground vibration decrease with an increase in joint angle.
- The ground vibration level increases with an increase in maximum charge per delay.
- Predicted PPV values from contour lines in O-PITBLAST are very close to the real data with the new attenuation law for OC-1, RGIII, SCCL, Telangana state, India.

References

[1] R.L. Ash, Ph.D. Thesis, The Influence of Geological Discontinuities on Rock Blasting, University of Minnesota, United States (1973).

[2] A.K. Hakan, Adnan Konuk, The effect of discontinuity frequency on ground vibrations produced from bench blasting: A case study. Soil Dyn. Earthq. **28** (9), 686-694 (2008). DOI: https://doi.org/10.1016/J.SOILDYN.2007.11.006

[3] B.S. Choudhary, K. Sonu, K. Kishore, S. Anwar, Effect of rock mass properties on blast-induced rock fragmentation. Int. J. Min. Miner. Eng. **7** (2), 89-101 (2016). DOI: https://dx.doi.org/10.1504/IJMME.2016.076489

[4] G.R. Adhikari, M.M. Singh, R.N. Gupth, Influence of rock properties on blast-induced vibration. Min. Sci. Technol. **8** (3), 297-300 (1989). DOI: https://doi.org/10.1016/S0167-9031(89)90437-4

[5] R.E. Goodman, Methods of Geological engineering in discontinuous Rock. West Publishing, St. Paul. (1976).

[6] M. King, L. Myerand, J. Rezowalli, Experimental studies of elastic-wave propagation in a columnar-jointed rock mass. Geophys. Prospect. **34**, 1185-1199 (1986). DOI: https://doi.org/10.1111/j.1365-2478.1986.tb00522.x

[7] G. Berta, Blasting-induced vibration in tunneling. unn. Undergr. Space Technol. (9), 175-187 (1994). DOI: https://doi.org/10.1016/0886-7798(94)90029-9

[8] S.P. Singh, The influence of geology on blast damage. CIM Bulletin, Conference: 26th International conference on ground control in mining At: Morgantown, West Virginia, USA (2007).

[9] R.E. Goodman, Block Theory and Its Application to Rock Engineering. Geotechnique. ISSN 0016-8505 | E-ISSN 1751-7656. **45** (3) 383-423 (1995). DOI: https://doi.org/10.1680/geot.1995.45.3.383

[10] P.R. La Pointe, H.G. Ganow, The influence of cleats and joints on production blast fragment size in the Wyodak Coal, Compbell Country, Wyoming, in Proceedings of the 27th US Symposium on Rock Mechanics, University of Alabama. pp. 464-70 (1986).

[11] D. Van Zyl, An approach to incorporate rock fabric information in blast fragmentation investigation. In Proceedings of the 2nd Mini-Symposium on Explosives and Blasting Research, Society of Explosives Engineers, Georgia. pp. 81-89 (1986).

[12] E.I. Efremov, V.M. Komir, N.I. Myachina, V.A. Nikiforova, S.N. Rodak, V.V. Shelenok, Influence of the structure of a medium on fragment size composition in blasting. Sov. Min. Sci. **16**, 18-22 (1980). DOI: https://doi.org/10.1007/BF02504281

[13] Y.K. Wua, H. Haoa, Y.X. Zhoub, K. Chongb, Propagation characteristics of blast-induced shock waves in a jointed rock mass. Soil Dyn. Earthq. Eng. **17**, 407-412 (1998). DOI: https://doi.org/10.1016/S0267-7261(98)00030-X

[14] W. Fourney, R.D. Dick, D.F. Fordyce, T.A. Weaver, Effects of Open Gaps on Particle Velocity Measurements. Rock Mech. Rock Eng. **30** (2), 95-111 (1997). DOI: https://doi.org/10.1007/BF01020127

[15] Rustan, Z.G. Yang, The influence from primary structure on fragmentation. 1st. International Symposium on rock fragmentation by blasting. Lulea, Sweden. **2**, 581-604 (1983).

[16] W.L. Fourney, Mechanisms of rock fragmentation in by blasting. Hudson J.A, editor. Compressive rock engineering, principles, practice and projects. Oxford: Pergamon Press (1993).

[17] R.K.Paswan, Mohammad. Sarim, P.K. Singh, H.S. Khare, B.K. Singh, R.J. Singh, Controlled blasting at Parsa East &KantaBasan opencast mines for safe and efficient Mining operations. Ind. Min. & Eng. J. **53** (4), 7-17 (2014).

[18] C.L. Jimeno, E. Jimeno, F.J.A. Carcedo, Drilling and Blasting of Rocks. A.A. Balkema Publishers, Rotterdam, The Netherlands. (1995). DOI: https://doi.org/10.1080/09208119608964786

[19] T.H. Lewandowski, V.K. Luan Mai, R.E. Danell. Influence of discontinuities on presplitting effectiveness, Rock fragmentation by blasting – Fragblast5. B. Mohanty, Montreal, Canada, (1996). DOI: https://doi.org/10.1080/13855149709408388

[20] P.N. Worsey, S. Qu. Effect of joint separation and filling on pre-split blasting. The 3rd Mini Symposium on Explosives and Blasting Research. pp. 26-40 (1987).

[21] B.S. Whittaker, R.N. Singh, G. Sun, Fracture Mechanics Applied to Rock Fragmentation due to blasting. Rock Fracture Mechanics – Principles, Design and Applications, Elsevier Science Ltd. **71** (13), 443-479 (1992).

[22] P.K. Singh, M.P. Roy, R.K. Paswan, Md. Sarim. Suraj Kumar, Rakesh Ranjan Jha, Rock fragmentation control in opencast blasting. J. Rock Mech. Geotech. **8**, 225-237 (2016). DOI: https://doi.org/10.1016/j.jrmge.2015.10. 005

[23] K. Nur Lyana, Z. Hareyani, A. Kamar Shah, Mohd, M.H. Hazizan, Effect of Geological Condition on Degree of Fragmentation in a Simpang Pulai Marble Quarry, 5th International Conference on Recent Advances in Materials, Minerals and Environment (RAMM) & 2nd International Postgraduate Conference on Materials, Mineral and Polymer (MAMIP), 4-6 August (2015).

[24] J.M. Belland, Structure as a Control in Rock Fragmentation Coal Lake Iron Ore Deposited. The Canadian Mining and Metallurgical Bulletin. **59** (647), 323-328 (1968).

[25] K. Talhi, B. Bensaker, Design of a model blasting system to measure peak p-wave stress, Soil Dyn. Earthq. Eng. **23** (6), 513-519 (2003). DOI: http://dx.doi.org/10.1016/S0267-7261(03)00018-6

[26] P.F. Gnirk, E.D. Fleider, On the correlation between explosive crater formation and rock properties. In Proceedings of the 9th Symposium on Rock Mechanics, AIME. New York. 321-45 (1968).

[27] D.P. Singh, Y.V. Apparao, S.S. Saluja, A laboratory study on effect of joints on rock fragmentation. American Rock Mechanics Association, The 21st U.S. Symposium of Rock Mechanics (USRMS), 27-30 May (1980).

[28] Zhi-qiang.Yin, Hu. Zu-xiang, Ze-di Wei, Guang-ming Zhao, Ma Hai-feng, Zhuo Zhang, Rui-min Feng, Assessment of Blasting-Induced Ground Vibration in an Open-Pit Mine under Different Rock Properties. Adv. Civ. Eng. 10 (2018). DOI: https://doi.org/10.1155/2018/4603687

[29] J. Henrych. The dynamics of explosion and its use. Earthq Eng Struct Dyn. Elsevier, New York (1979). DOI: https://doi.org/10.1002/eqe.4290080309

[30] G.W. Ma, X.M. An, Numerical simulation of blasting-induced rock fractures. Int. J. Rock Mech. Min. Sci. **45** (6), 966-975 (2008). DOI: http://dx.doi.org/10.1016/j.ijrmms.2007.12. 002

[31] J.C. Li, W. MaG., Analysis of blastwave interaction with a rock joint. Rock Mech Rock Eng. **43** (6), 777-787 (2010). DOI: https://doi.org/10.1007/s00603-009-0062-0

[32] J.C. Li, H.B. Li, J. Zhao, An improved equivalent viscoelastic medium method for wave propagation across layered rock masses. Int. J. Rock Mech. Min. Sci. (2015). DOI: http://dx.doi.org/10.1016/j.ijrmms.2014.10.008

[33] P.C. Vinh, T.T. Tuan, D.X. Tung, N.T. Kieu, Reflection and transmission of SH waves at a very rough interface and its band gaps. J. Sound Vib. 411-422 (2017). DOI: https://doi.org/10.1016/j.jsv.2017.08.046